Commun. **2000**, *271*, 334–336; b) J. von Lintig, K. Vogt, *J. Biol. Chem.* **2000**, *275*, 11915–11920; c) A. Wyss, G. Wirtz, W.-D. Woggon, R. Brugger, M. Wyss, A. Friedlein, H. Bachmann, W. Hunziker, *Biochem. J.* **2001**, *354*, 521–529.

[11] G. M. Wirtz, C. Bornemann, A. Giger, R. K. Müller, H. Schneider, G. Schlotterbeck, G. Schiefer, W.-D. Woggon, *Helv. Chim. Acta* **2001**, in press.

[12] J. Rétey, A. Umani-Ronchi, J. Seibel, D. Arigoni, *Experientia* **1966**, *22*, 502–503.

[13] J. Devery, B. V. Milborrow, *Br. J. Nutr.* **1994**, *72*, 397–414.

[14] a) R. R. French, P. Holzer, M. G. Leuenberger, W.-D. Woggon, *Angew. Chem.* **2000**, *112*, 1321–1323; *Angew. Chem. Int. Ed.* **2000**, *39*, 1267–1269; b) W.-D. Woggon, *Chimia* **2000**, 57; c) R. R. French, J. Wirz, W.-D. Woggon, *Helv. Chim. Acta* **1998**, *81*, 1521–1527.

[15] C. Engeloch-Jarret, M. G. Leuenberger, W.-D. Woggon, unpublished results.

[16] G. J. Handelman, M. J. Haskell, A. D. Jones, A. J. Clifford, *Anal. Chem.* **1993**, *65*, 2024–2028.

Saddle-Shaped Six-Coordinate Iron(III) Porphyrin Complexes Showing a Novel Spin Crossover between $S = 1/2$ and $S = 3/2$ Spin States**

Takahisa Ikeue, Yoshiki Ohgo, Tatsuya Yamaguchi,
Masashi Takahashi,* Masuo Takeda, and
Mikio Nakamura*

Spin states of iron(III) porphyrins are controlled by the number and nature of axial ligands.[1] The coordination of nitrogen bases such as imidazole (HIm) and pyridine results in the formation of low-spin ($S = 1/2$) six-coordinate complexes. In contrast, anionic ligands such as Cl^- and F^- lead to the formation of five-coordinate high-spin ($S = 5/2$) complexes. Maltempo discussed a spin-admixed $S = 3/2$, $5/2$ state on the basis of quantum mechanical calculations, and suggested that the $S = 3/2$ state is an important contributor to the spin state of certain bacterial heme proteins known as cytochromes c′.[2] We and others recently reported that highly nonplanar (porphyrinato)iron(III) complexes with weak axial ligands show a quite pure intermediate spin state.[3, 4] The results were ascribed to the short $Fe{-}N_{por}$ bonds of the nonplanar porphyrin rings and the weak coordination ability of the axial ligands.[5] We therefore expected that the spin state of nonplanar $[Fe^{III}(oetpp)L_2]ClO_4$ (**1**–**5**) could change from the pure $S = 1/2$ to the pure $S = 3/2$ state as the axial ligand changes from strong HIm to weak THF; the order of the coordination ability is HIm > dmap > py > 4-CNpy > thf.[6] Of particular interest are the spin states of **2**–**4** because the axial ligands of these complexes are ranked between HIm and THF.

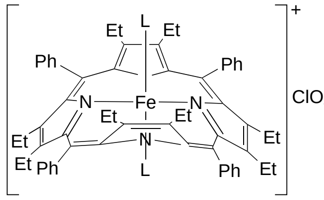

1: L = HIm
2: L = dmap
3: L = py
4: L = 4-CNpy
5: L = thf

$[Fe(Oetpp)L_2]ClO_4$

Table 1 lists the Mössbauer parameters, isomer shift (IS; relative to α-iron foil at 290 K), and quadrupole splitting (QS) measured at ambient and liquid nitrogen temperatures. The QS values for **1** and **2** at ambient temperature were within the range of low-spin complexes.[7] The IS and QS values for **4** (0.37 and 3.26 mm s^{-1}, respectively) were close to those for **5** (0.41 and 3.65 mm s^{-1}); **5** has been fully characterized as the quite pure intermediate-spin complex.[4] Thus, from the viewpoint of Mössbauer spectroscopy, **1** and **2** are the low-spin complexes, while **4** is the intermediate-spin complex at ambient temperature. Figure 1 shows the Mössbauer spectra of **3** and **4** taken at ambient temperature and 80 K. The features change as the temperature is lowered. Complex **4** exhibited a new doublet (site B) below 230 K, and the relative intensities for this site increased on decreasing the temperature. The values for sites A and B are in the range of intermediate-spin and low-spin complexes, respectively, and both spin states co-exist at low temperature. This observation implies the occurrence of a novel spin-crossover process [Eq. (1)].[8, 9]

Table 1. Mössbauer parameters and spin state (S) of **1**–**5**.

		T [K]	IS [mm s^{-1}]	QS [mm s^{-1}]	Γ_1 [mm s^{-1}]	Γ_2 [mm s^{-1}]	S
1		297	0.18	1.82	0.24	0.25	1/2
		78	0.26	1.86	0.40	0.62	1/2
2		290	0.19	2.21	0.27	0.32	1/2
		80	0.26	2.31	0.55	0.89	1/2
3		290	0.32	2.76	0.27	0.29	3/2–1/2
		80	0.25	2.29	0.47	0.64	1/2
4	site A	295	0.37	3.26	0.32	0.33	3/2
	site A	80	0.57	3.03	0.47	0.47	3/2
	site B	80	0.20	2.70	0.64	0.64	1/2
5		290	0.41	3.65	0.32	0.26	3/2
		80	0.50	3.50	0.77	0.49	3/2

$$\text{low spin } (S = 1/2) \rightleftharpoons \text{intermediate spin } (S = 3/2) \qquad (1)$$

---

[*] Prof. Dr. M. Nakamura, Dr. T. Ikeue, Dr. Y. Ohgo, T. Yamaguchi
Department of Chemistry
Toho University School of Medicine
Tokyo 143-8540 (Japan)
Fax: (+81) 3-5493-5430
E-mail: mnakamu@med.toho-u.ac.jp

Prof. Dr. M. Takahashi, Prof. Dr. M. Takeda
Department of Chemistry
Faculty of Science, Toho University
Funabashi, 274-8510 (Japan)
Fax: (+81) 47-475-1855
E-mail: takahasi@chem.sci.toho-u.ac.jp

[**] This work was supported by a Grant in Aid for Scientific Research on Priority Areas (A; no. 12020257 to M.N.) from the Ministry of Education, Culture, Sports, Science, and Technology, Japan. T.I. is grateful to the JSPS for a Research Fellowship for young scientists. We thank the Research Center for Molecular Materials, the Institute for Molecular Science (IMS), for support. The authors are grateful to Mr. Masahiro Sakai of the IMS for the assistance with the SQUID measurements.

Supporting information for this article is available on the WWW under http://www.angewandte.com or from the author.

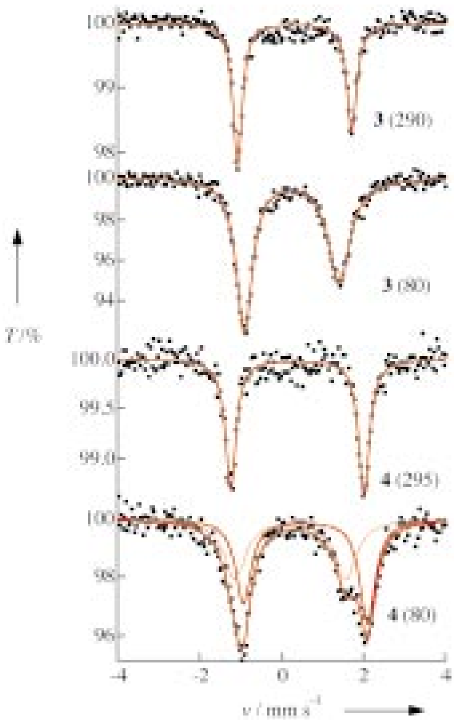

Figure 1. ^{57}Fe Mössbauer spectra of **3** and **4** measured on microcrystalline samples at ambient temperature and 80 K (as indicated in the parentheses).

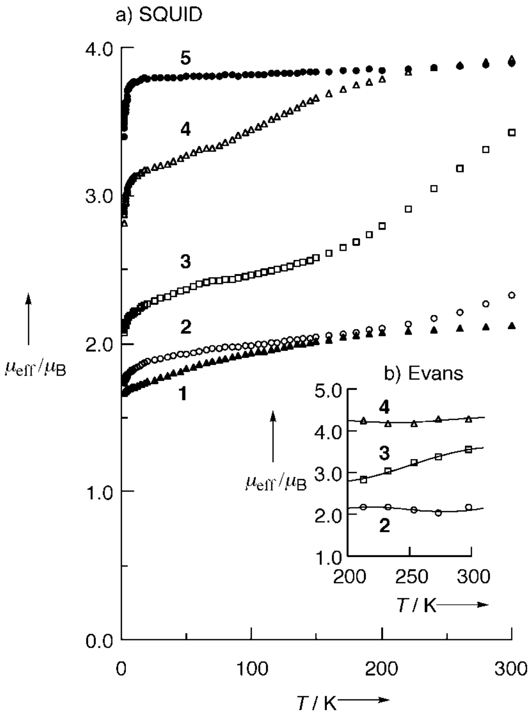

Figure 2. Temperature dependence of the effective magnetic moments of **1**–**5** taken for microcrystalline samples by SQUID magnetometry. Inset: Effective magnetic moments determined in CH_2Cl_2 by the Evans method.

While **4** exhibited a new doublet at low temperature, **3** maintained a set of doublets throughout the temperature range measured. The IS and QS values of **3**, however, showed an unexpected decrease on lowering the temperature and were almost the same as those of **2** below 150 K. This result suggests that **3** exists as the low-spin state below 150 K. Since, however, the IS and QS values of **3** at ambient temperature were close to those of intermediate-spin complexes, it is also considered to be a spin-crossover complex. The observation of only one set of doublets in **3** could be explained in terms of the fast spin transition on the Mössbauer time scale (10^7 s^{-1}) over 150–290 K when two iron sites are present.

Figure 2 shows the effective magnetic moments (μ_{eff}) of microcrystalline samples measured with a SQUID magnetometer over 2–300 K. The results confirm that **1** and **2** are in the $S = 1/2$ state. A major part of **3** is in the $S = 1/2$ state below 150 K, but the population of the $S = 3/2$ state considerably increases above this temperature. Similarly, **4** is a mixture of the $S = 1/2$ and $S = 3/2$ states below 200 K, although it exists almost exclusively as the $S = 3/2$ complex above 200 K. These results support the occurrence of the spin-crossover process [Eq. (1)] in **3** and **4**, as suggested by the Mössbauer spectroscopy results. As mentioned, **5** is a quite pure intermediate-spin complex as shown by the μ_{eff} value being maintained at 3.80 ± 0.09 μ_B in the range 5–300 K.[4] The EPR spectra taken for the solid samples at 4.2 K are consistent with the conclusions obtained from the Mössbauer spectroscopy and SQUID magnetometry measurements.[10]

The spin states of these complexes in solution have been studied. The solution magnetic moments (inset, Figure 2) were determined by the Evans method over the temperature range 193–298 K. The μ_{eff} values of **2** and **4** were almost constant, 2.1 ± 0.1 and 4.2 ± 0.1 μ_B, respectively, which are close to the spin-only values expected for the $S = 1/2$ and $S = 3/2$ complexes, respectively. As in the case of the solid sample, the μ_{eff} value of **3** in solution decreased from 3.5 μ_B (298 K) to 2.6 μ_B (193 K), which suggests the spin-crossover process also occurs in solution. Table 2 shows the ^1H NMR chemical shifts at 223 K. The large downfield shifts of the CH_2 and ligand (L) signals on going from **2** to **4** suggest that the spin densities at the β-pyrrole and the ligand carbon atoms increase from **2** → **4**. The result can be explained in terms of the increase in population of the $S = 3/2$ state relative to that of the $S = 1/2$ state.[4] Table 3 shows the ^{13}C NMR chemical shifts at 223 K.[11] The most characteristic feature is the large upfield shift of the *meso* carbon atom (C–Ph) on going from **2** ($\delta = -28$) to **4** ($\delta = -451$); the chemical shift of the *meso* carbon atom at $\delta = -451$ ($\delta = -235$ at 298 K) is unprecedented in ^{13}C NMR spectroscopy of iron(III) porphyrins, and suggests that the major part of **4** is in the $S = 3/2$ state.[12–14] Thus, the observation of the extremely upfield-shifted signal of the *meso* carbon atom by ^{13}C NMR spectroscopy could be a good proof for the intermediate-spin complex.[15] In fact, the pure intermediate-spin complex **5** also showed the signal corre-

Table 2. ^1H NMR chemical shifts recorded in CD_2Cl_2 at 223 K.

	L	*meso* Phenyl			Pyrrole		Axial ligand
		o	*m*	*p*	CH_2	CH_3	ring protons
1	HIm	2.8	4.7	6.0	3.2, 11.8	1.3	
2	dmap	3.2	4.8	6.0	3.4, 12.5	1.3	15.8, −2.7
3	py	8.5	5.1	8.5	8.2, 27.9	0.3	35.9, 29.6
4	4-CNpy	14.4	4.2	13.7	19.3, 55.5	−1.7	113.7, 72.5

Table 3. ^{13}C NMR chemical shifts recorded in CD_2Cl_2 at 223 K.

	L	*meso*	*ipso*	*o*	*m*	*p*	Pyrrole (α)	Pyrrole (β)	CH_2	CH_3
1	HIm	– 37	166	97	122	123	143	156	– 38	105
2	dmap	– 28	159	102	122	123	132	164	– 40	102
3	py	– 135	249	31	124	119	284	223	– 53	162
4	4-CNpy	– 451	458	– 160	130	105	590	304	– 80	264

sponding to the *meso* carbon atom to be fairly upfield shifted ($\delta = -265$ at 223 K).[16]

Figure 3 shows the temperature dependence of the ^{13}C chemical shifts of the *meso* carbon atoms. While the chemical shift of the meso carbon atom of **3** was quite similar to that of **4** at 298 K, the value approached that of **2** at 200 K. Since **2** and **4** are considered to be the pure $S = 1/2$ and $S = 3/2$ complexes, respectively, in this temperature range, the spin-crossover constant K_{sc} of **3** is calculated according to Equation (2).

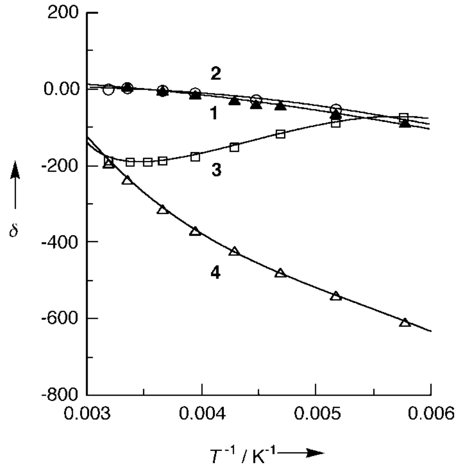

Figure 3. Temperature dependence of the chemical shifts of the *meso* ^{13}C atoms of **1**–**4** taken in CD_2Cl_2.

$$K_{sc} = (\delta_{dmap} - \delta_{py})/(\delta_{py} - \delta_{4\text{-}CNpy}) \qquad (2)$$

The plots of log(K_{sc}) versus $1/T$ showed a good linear relationship, from which the thermodynamic parameters were obtained as $\Delta H = 16.9\,kJ\,mol^{-1}$ and $\Delta S = 66.6\,J\,mol^{-1}\,K^{-1}$. Although the spin-crossover process between the $S = 1/2$ and $S = 3/2$ states is not unprecedented in iron(III) complexes,[8, 9] this is, to the best of our knowledge, the first example in iron(III) porphyrin complexes.

It is interesting to compare the spin state of saddle-shaped **4** with that of ruffled $[Fe^{III}(TiPrP)(4\text{-}CNPy)_2]ClO_4$.[6] Although both complexes are supposed to have short $Fe{-}N_{por}$ bonds as a result of the deformation of the porphyrin ring, $[Fe^{III}(TiPrP)(4\text{-}CNPy)_2]ClO_4$ is in the low-spin state with a $(d_{xz}, d_{yz})^4(d_{xy})^1$ electron configuration.[14] The result is ascribed to the difference in the energy gap between the d_{z^2} and d_π orbitals; the energy gap is larger in $[Fe^{III}(TiPrP)(4\text{-}CNPy)_2]ClO_4$ than in **4** since the d_π orbitals of the former complex is located below the d_{xy} orbital. In addition, the coordination of 4-CNPy is much stronger in the ruffled complex than in saddle-shaped **4** for steric reasons, which further increases the energy gap.[17] Consequently, $[Fe^{III}(TiPrP)(4\text{-}CNPy)_2]ClO_4$ maintains the low-spin state. If 4-CNpy is replaced by thf, both saddle-shaped **5** and ruffled $[Fe^{III}(TiPrP)(thf)_2]ClO_4$ show quite pure intermediate-spin characteristics.[4]

In conclusion, we have shown that the saddle-shaped complexes $[Fe^{III}(oetpp)L_2]ClO_4$ exhibit a novel spin-crossover process between the $S = 1/2$ and $S = 3/2$ states, and that the $S = 3/2$ population increases as the coordination ability of the axial ligand is weakened. It should be emphasized here that the novel spin-crossover process in six-coordinate iron(III) porphyrins is realized by the tremendous deformation of the porphyrin rings. The large destabilization of the $d_{x^2-y^2}$ orbital caused by the short $Fe{-}N_{por}$ bonds insulates the $S = 5/2$ state from the other electronic ground states. The spin state of the iron(III) ions can hence be finely tuned by the field strength of the axial ligands, thus leading to the formation of the complex with the pure $S = 1/2$ state (**1**), complexes showing the novel $S = 1/2 \rightleftharpoons S = 3/2$ process (**2**–**4**), and the complex with the pure $S = 3/2$ state (**5**).

Experimental Section

$[Fe^{III}(oetpp)Cl]$ and *meso*-^{13}C-enriched $[Fe^{III}(oetpp)Cl]$ were prepared according to the literature.[18, 19]

5: A solution (15 mL) of $AgClO_4$ (6.1 mg, 2.9×10^{-5} mol) in THF was added to a dry solution of $[Fe^{III}(oetpp)Cl]$ (26.1 mg, 2.8×10^{-5} mol) in THF (20 mL). After the removal of AgCl by filtration, heptane (20 mL) was added, and the solution was allowed to stand overnight. The purple crystals were collected by filtration, washed with hexane, and dried in vacuo for 10 min at 25 °C to give 25 mg (87 %) of **5**, which was characterized as the quite pure intermediate-spin complex.[4] **1**–**4** were prepared by the addition of an excess amount of ligand to a solution of **5** in CH_2Cl_2 followed by recrystallization from CH_2Cl_2/heptane. The ^1H and ^{13}C NMR data are shown in Tables 1 and 2, respectively.

The ^1H and ^{13}C NMR spectra were recorded on a JEOL LA300 spectrometer operating at 300.4 MHz for proton spectroscopy. EPR spectra were recorded on a Bruker E500 spectrometer operating at the X band and equipped with an Oxford helium cryostat. The solid-state magnetic susceptibilities were measured between 2 and 300 K under a magnetic field of 0.5 T with a SQUID magnetometer (Quantum Design MPMS-7). The measured data were corrected for diamagnetic contributions. Iron-57 Mössbauer spectra were measured on a Wissel Mössbauer spectrometer system. The samples were kept in a gas-flow cryostat and the $^{57}Co(Rh)$ source was kept at room temperature. Isomer shifts (δ) are given relative to α-iron foil at room temperature.

Received: February 5, 2001
Revised: May 7, 2001 [Z16551]

---

[1] W. R. Scheidt in *The Porphyrin Handbook*, *Vol. 3* (Eds.: K. M. Kadishi, K. M. Smith, R. Guilard), Academic Press, San Diego, **2000**, pp. 49–112.

[2] M. M. Maltempo, *J. Chem. Phys.* **1974**, *61*, 2540–2547.

[3] J.-P. Simonato, J. Pecaut, L. L. Pape, J.-L. Oddou, C. Jeandey, M. Shang, W. R. Scheidt, J. Wojacynski, S. Wolowiec, L. Latos-Grazynski, J.-C. Marchon, *Inorg. Chem.* **2000**, *39*, 3978–3987.

[4] T. Ikeue, T. Saitoh, T. Yamaguchi, Y. Ohgo, M. Nakamura, M. Takahashi, M. Takeda, *Chem. Commun.* **2000**, 1989–1990.

[5] D. R. Evans, C. A. Reed, *J. Am. Chem. Soc.* **2000**, *122*, 4660–4667.

[6] Abbreviations: oetpp, T*i*PrP, and TEtP are dianions of 2,3,7,8,12,13,17,18-octaethyl-5,10,15,20-tetraphenylporphyrin, *meso*-tetraisopropylporphyrin, and *meso*-tetraethylporphyrin, respectively. dmap: 4-dimethylaminopyridine; py: pyridine; 4-CNpy: 4-cyanopyridine; HIm: imidazole; 2-MeIm: 2-methylimidazole.

[7] J. Sams, T. B. Tsin in *The Porphyrins*, *Vol. IV* (Ed.: D. Dolphin), Academic Press, New York, **1979**, pp. 425–478.

[8] K. D. Hodges, R. G. Wollmann, S. L. Kessel, D. N. Hendrickson, D. G. Van Derveer, E. K. Barefield, *J. Am. Chem. Soc.* **1979**, *101*, 906–917.

[9] W. O. Koch, V. Schünemann, M. Gerdan, A. X. Trautwein, H.-J. Krüger, *Chem. Eur. J.* **1998**, *4*, 686–691.

[10] EPR measurements: **1:** $g = 2.79, 2.35, 1.63$ ($S = 1/2$); $g = 3.25$ ($S = 1/2$). **2:** $g = 3.06, 2.14, 1.42$ ($S = 1/2$). **3:** $g = 3.39, 2.08$ ($S = 1/2$). **4**: $g = 4.28, 3.80, 2.08$ ($S = 3/2$).

[11] The signals corresponding to the *meso* carbon atoms were assigned unambiguously by the use of *meso*-^{13}C-enriched complexes. The α-pyrrole and *ipso*-phenyl signals were assigned on the basis of their coupling with the *meso* carbon atom of the labeled complexes.

[12] High-spin and low-spin complexes show *meso* signals at $\delta = 500–600$ and 50–100, respectively, at room temperature.[13] Some low-spin complexes with the less common $(d_{xz}, d_{yz})^4(d_{xy})^1$ electronic configuration exhibit the signals further downfield ($\delta = 700–800$).[14]

[13] "Physical Bioinorganic Chemistry Series 1": H. Goff in *Iron Porphyrin*, *Part I* (Eds.: A. B. P. Lever, H. B. Gray), Addison-Wesley, Reading, **1983**, pp. 237–281.

[14] T. Ikeue, Y. Ohgo, T. Saitoh, M. Nakamura, H. Fujii, M. Yokoyama, *J. Am. Chem. Soc.* **2000**, *122*, 4068–4076.

[15] The large downfield shifts of the α- and β-pyrrole signals are consistent with the occupancy of unpaired electrons in both the d_{xz} and d_{yz} orbitals; the unpaired electrons in these orbitals are transferred to the pyrrole carbon atoms by a d_π-$3e_g$ interaction. Since the $3e_g$ orbital has zero electron density at the *meso* carbon atom, the large upfield shift of the *meso* signal is ascribed to the spin polarization from the neighboring α-pyrrole carbon atom.[14]

[16] The extent of the upfield shift of the *meso* carbon atom is not necessarily proportional to the $S = 3/2$ contribution. The large difference in the shifts of the *meso* carbon atoms between **4** and **5** ($\Delta\delta = 186$ at 223 K) could be the indication that the d_π-$3e_g$ interaction in **4** is much stronger than that in **5** as a result of the difference in the nature of the axial ligands.

[17] Although the X-ray crystal structures of **4** and [Fe^{III}(T*i*PrP)(4-CNpy)$_2$]ClO$_4$ are not available at present, a preliminary result has shown that saddled **3** has much longer Fe–N(axial ligand) bonds than ruffled [Fe^{III}(TEtP)(2-MeIm)$_2$]Cl; the average bond lengths are 2.203(3) and 2.02(1) Å, respectively. Y. Ohgo, T. Ikeue, M. Nakamura, unpublished results.

[18] K. M. Barigia, M. D. Berber, J. Fajer, C. J. Medforth, M. W. Renner, K. M. Smith, *J. Am. Chem. Soc.* **1990**, *112*, 8851–8857.

[19] R.-J. Cheng, P.-Y. Chen, P.-R. Gau, C.-C. Chen, S.-M. Peng, *J. Am. Chem. Soc.* **1997**, *119*, 2563–2569.

Molecular Paneling by Coordination: An $M_{15}L_6$ Hexahedral Molecular Capsule having Clefts for Reversible Guest Inclusion

Kazuhiko Umemoto, Hitoshi Tsukui,
Takahiro Kusukawa, Kumar Biradha, and
Makoto Fujita*

The construction of three-dimensional (3D) molecular structures by linking two-dimensional (2D), planar organic components through metal coordination provides a new concept that is termed molecular paneling.[1] A family of 2D components are coordinated by transition metals to give rise to various hollow 3D polyhedral structures.[2–8] The triangular *exo*-hexadentate ligand **2** has been recently shown to give $M_{18}L_6$ hexahedral coordination capsule **4** by linking together with Pd^{II} building block **1**.[4b] This coordination capsule has a very stable closed-shell structure which makes it difficult to encapsulate guest molecules. We have designed another molecular panel **3**, which is similar to **2** but misses one binding site, to prepare a hexahedral capsule with more

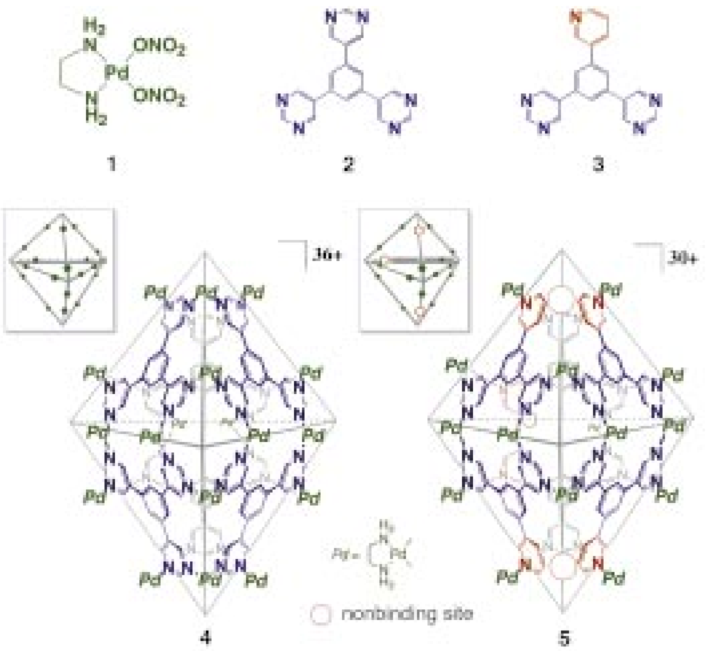

---

[*] Prof. Dr. M. Fujita,[+] H. Tsukui, Dr. T. Kusukawa, Dr. K. Biradha
Department of Applied Chemistry
Graduate School of Engineering, Nagoya University
Chikusaku, Nagoya 464-8603 (Japan)
Fax: (+81) 52-789-3199
E-mail: mfujita@apchem.nagoya-u.ac.jp

Dr. K. Umemoto
The Graduate University for Advanced Studies
Myodaiji, Okazaki 444-8585 (Japan)

[+] Prof. Fujita is responsible for the Core Research for Evolutional Science and Technology (CREST) project of the Japan Science and Technology Corporation (JST).

Supporting information for this article is available on the WWW under http://www.angewandte.com or from the author.